ACADEMIC
PRESS

Changing moisture sources over the last 330,000 years in Northern Oman from fluid-inclusion evidence in speleothems

Dominik Fleitmann,[a,]* Stephen J. Burns,[b] Ulrich Neff,[c] Augusto Mangini,[c]
and Albert Matter[a]

[a] *Institute of Geological Sciences, University of Bern, Baltzerstrasse 1-3, 3012 Bern, Switzerland*
[b] *Department of Geosciences, Morrill Science Center, University of Massachusetts, Amherst, MA 01002, USA*
[c] *Heidelberg Academy of Sciences, Im Neuenheimer Feld 229, 69120 Heidelberg, Germany*

Abstract

Speleothems from Hoti Cave in northern Oman provide a record of continental pluvial periods over the last 330,000 yr. Periods of rapid speleothem deposition occurred from 6000 to 10,500, 78,000 to 82,000, 120,000 to 135,000, 180,000 to 200,000, and 300,000 to 330,000 yr ago, with little or no growth during the intervening periods. During each of these five pluvial periods, δD values of water extracted from speleothem fluid inclusions (δD_{FI}) are between -60 and $-20‰$ (VSMOW) and $\delta^{18}O$ values of speleothem calcite ($\delta^{18}O_C$) are between -12 and $-4‰$ to (VPDB). These values are much more negative than modern rainfall (for δD) or modern stalagmites (for $\delta^{18}O$). Previous work on the isotopic composition of rainfall in Oman has shown that northern and southern moisture sources are isotopically distinct. Combined measurements of the δD values of fluid-inclusion water with calculated $\delta^{18}O$ values from peak interglacial speleothems indicate that groundwater was predominantly recharged by the southern (Indian Ocean) moisture source, when the monsoon rainfall belt moved northward and reached Northern Oman during each of these periods.
© 2003 University of Washington. Published by Elsevier Inc. All rights reserved.

Keywords: Speleothems; Stable isotopes; Fluid inclusions; Paleoprecipitation; Oman

Introduction

Currently, information on climate variability on glacial-interglacial time scales in the areas that border the Arabian Sea comes almost entirely from marine cores (Van Campo et al., 1982; Clemens and Prell, 1990; Clemens et al., 1991; Anderson and Prell, 1993). Paleoclimatic information obtained from marine records is based on various proxies, such as the percentage of *Globigerinoides bulloides* (a foraminifer associated with upwelling water), trace element concentrations (e.g., barium or silica) and aeolian lithogenic grain sizes. All of these proxies, however, are rather an indicator of monsoonal wind strength than of continental wetness. Terrestrial paleoclimate records, such as paleolake sediments and dune deposits, are more suitable to monitor

fluctuations in the hydrological cycle in Northern Africa and on the Arabian Peninsula. Long-term records, however, are scarce and widely distributed geographically. Even when paleolake sequences are preserved (e.g., Szabo et al., 1995), precise Uranium-series age dating has not been possible due to diagenetic effects and detrital contamination, both of which result in large age uncertainties. Moreover, while paleolake sequences and dune deposits (e.g., Preusser et al., 2002) may reveal the occurrence of pluvial periods and/or wind direction, they do not give direct information about the source of precipitation. In contrast to these terrestrial paleoclimate archives, speleothems (stalagmites, stalactites, and flowstones) may provide direct information on the isotopic composition of rainfall and, therefore, potentially identify the source of moisture to a given area. The oxygen isotope ratios of speleothem calcite ($\delta^{18}O_C$) and hydrogen isotope ratios of speleothem fluid inclusion (δD_{FI}) are water-isotope tracers, which enable the calculation of the isotopic com-

* Corresponding author. Fax: +0049-0-31-631-48-43.
E-mail address: dominik.fleitmann@geo.unibe.ch (D. Fleitmann).

position of paleogroundwater and paleoprecipitation. Knowledge of the isotopic composition of paleoprecipitation in Northern Oman helps to better identify changes in the moisture source, air mass trajectories, and rain-out history on glacial-interglacial time scales.

A composite oxygen isotope record derived from speleothems at Hoti Cave in Northern Oman and dated by uranium-series indicates five periods of increased wetness occurring at 6000–10,500, 78,000–82,000, 120,000–135,000, 180,000–200,000, and 300,000–325,000 yr ago (Burns et al., 1998, 2001). It has been suggested that during each of these periods the intertropical convergence zone (ITCZ) moved north into the Arabian Peninsula and that the Indian Ocean monsoon reached Northern Oman (Burns et al., 1998, 2001; Neff et al., 2001). Currently, this interpretation is based on the highly negative character of $\delta^{18}O_C$ values alone. An additional indicator of rainfall isotopic composition is the hydrogen isotopic composition of speleothem fluid inclusions, which are filled with water that was trapped in the host calcite at the time of growth (Schwarcz et al., 1976, Kendall and Broughton, 1978). Provided that evaporation within the cave has not affected the drip waters, fluid inclusions preserve the isotope composition of cave drip water and groundwater, respectively. Due to the fact that in many caves the isotopic composition of drip waters reflects the isotopic composition of mean annual precipitation at the cave site (Harmon et al., 1979; Yonge et al., 1985), direct information about the hydrogen isotope composition of precipitation can be gained. Finally, in combination with $\delta^{18}O_C$ values and estimated cave temperatures, the isotope composition of paleogroundwater and paleoprecipitation can be reconstructed.

Currently, two methods are used to liberate water from speleothem fluid inclusions for hydrogen isotope analysis: (1) by thermal decrepitation at high temperatures (Yonge, 1982; Matthews et al., 2000) and (2) by crushing under high vacuum at low temperatures (Dennis et al., 1997, 2001). The first method, thermal decrepitation, liberates fluid-inclusion water at very high temperatures (400° to 500°C). However, fluid-inclusion water extracted and recovered from active stalagmites using this method is −20 to −30‰ (VSMOW) more depleted than their parent drip waters, and, thus, a correction is needed (Yonge, 1982; Matthews et al., 2000). Furthermore, thermal decrepitation releases large volumes of CO_2, hindering precise measurements of fluid inclusion oxygen isotopes. To avoid the problems associated with the thermal decrepitation method a vacuum-crushing cell was designed by Dennis et al. (1997). Recent studies have shown that the crushing method enables simultaneous measurements of the isotopic composition of fluid-inclusion water with a precision of ±3‰ for δD and ±0.4‰ for $\delta^{18}O$ without any analytical fractionation (Dennis et al., 1997, 2001).

Despite these results, the reliability of $\delta^{18}O$ measurements of speleothem fluid inclusions is still a subject of ongoing discussions, because of possible postdepositional oxygen isotope exchange between inclusion water and spe-
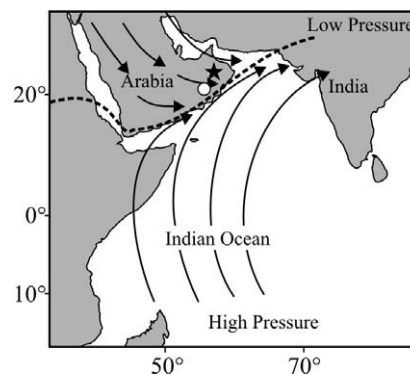

Fig. 1. Location map of Hoti Cave (black star), arrows indicate generalized modern, summer surface-wind patterns. Dashed line is the approximate position of the intertropical convergence zone (ITCZ), which roughly marks the northern limit of monsoon rainfall. The white circle marks the Al Wusta area.

leothem calcite over time (Schwarcz et al., 1976). However, hydrogen isotopes do not exchange with their calcite host rock and, therefore, accurately reflect the hydrogen isotopic composition of cave drip water and precipitation. In this paper we present the results of hydrogen isotope measurements of fluid inclusion from uranium-series dated speleothems from Hoti Cave in Northern Oman, which provide direct information about the moisture source of precipitation and, thus, paleo-wind directions during the last 330,000 yr.

Environmental settings

Hoti Cave (57° 21′ E, 23° 05′ N) is located in Northern Oman, in the foothills along the southern margin of the Oman Mountains (Fig. 1). The cave system, hosted in the Cretaceous limestone of the Natih Formation, has two entrances and is a subsurface, 4.5-km-long wadi. The cave air temperature is variable near both entrances and is more constant at approximately 26°C inside. The present climate of the area is arid to semiarid with an annual precipitation ranging from 50 to 255 mm yr^{-1} (station AI Hamra, 700 m above sea level, 1974–1997). Mean monthly temperatures range from 33° to 35°C during the summer months and from 20° to 25°C during the winter months. Precipitation in Northern Oman is extremely variable and originates from three sources. The first source is Mediterranean frontal systems approaching from the northwest, occurring mostly between December and March. The second source of precipitation is local thunderstorms, which form over the Jabal Akhdar mountains during very hot summers (orographic rain). These thunderstorms cause short and heavy rainfall. The third source of precipitation is tropical cyclones, which originate in the Bay of Bengal and the southeastern Arabian Sea. Tropical cyclones reach Northern Oman once every 5 to 10 yr (Pedgely, 1989) between the summer and the winter season (May–June and October–November) and are associ-

ated with heavy rainfalls of several days duration. At present, Northern Oman is not affected by the Indian Ocean monsoon, because the intertropical convergence zone and the associated monsoon rainfall belt remains generally to the south of the Arabian Peninsula (Hastenrath, 1985) (Fig. 1).

Sample description

Eight stalagmites and one flowstone were collected in Hoti Cave as whole samples or by drilling. The height of the fossil stalagmites ranges from about 0.6 to 3.0 m. Active stalagmites are almost absent in Hoti Cave; most of them are smaller than 0.3 m. Only one large active stalagmite was found in the entire cave, the 1-m-long stalagmite H12.

Thin sections were studied from all samples to investigate the nature of speleothem fluid inclusions. Most fluid inclusions are ellipsoidal or sausage-shaped micrometer-size cavities ranging from 1 to 20 μm. The majority of the cavities are completely filled with water; two-phase inclusions (gas-water) are rare. In general, these cavities tend to form inclusion-rich bands.

Analytical methods

Uranium-series dating

Ages were determined by measuring the U/Th ratios of the samples by thermal ionization mass spectrometry; a total of 86 measurements were made for all samples (see Table 1). Analytical procedures for the separation and purification of thorium and uranium follow closely those described in detail by Ivanovich and Harmon (1993). U/Th measurements were performed on a multicollector mass spectrometer (Finnigan MAT 262 RPQ) with a double filament technique. Uranium and thorium were measured in semi-peak-jump mode and peak-jump mode, respectively. Calibration of Faraday Cup to ICM efficiency was made by adopting the natural ratio $^{238}U/^{235}U$ of 137.88. To determine the uranium and thorium concentrations, defined quantities of a $^{233}U/^{236}U$ double spike and a ^{229}Th spike were added. Th/U ages were corrected for detritus following Ivanovich and Harmon (1993) assuming a $^{232}Th/^{238}U$ isotope ratio of 3.8. The reproducibility of the isotope ratio of $^{234}U/^{238}U$ and the concentration of ^{232}Th of standard materials is 0.3% and 0.8% (2σ), respectively. For details about measurements of the standard material, see Frank et al. (2000).

Oxygen isotope measurements

More than 2800 oxygen and carbon isotope analyses were done on all speleothems sampled in Hoti Cave (Burns et al., 1998, 2001; Neff et al., 2001; Fleitmann, 2001). The oxygen isotopes shown in this paper are a representative selection. For isotopic analyses approximately 5 mg of powder was drilled from the sample and analyzed with an on-line, automated, carbonate preparation system linked to a VG Prism II isotope ratio mass spectrometer. Results of these analyses are shown as the per-mil deviation between the sample and the Vienna Pee Dee Belemnite standard (VPDB) in delta notation. Reproducibility of standard materials is 0.08‰. Drip-water δD and $\delta^{18}O$ values were measured using an on-line, automated equilibration system. The values are reported against Vienna standard mean ocean water (VSMOW) and have a reproducibility of ±0.6‰ for hydrogen and ±0.1‰ for oxygen.

Hydrogen isotope measurements on speleothem fluid inclusions

The high-vacuum-crushing cell is a metal construction with copper con-flat seals. An internal hammer, driven by an external electromagnetic coil, is repeatedly raised and dropped onto the sample (Dennis et al., 1997). The sample, varying between 1.5 and 2.5 g, is placed in the cell and evacuated until a vacuum, higher than 1×10^{-4} mb, is achieved. Thereafter, the vacuum-crushing cell is isolated from the vacuum manifold and opened to a cold trap, cooled with liquid nitrogen ($-190°C$). The sample is crushed using 100–150 impact cycles and the crushing cell is then heated to 150°C to transfer the liberated water over a period of 60 min to a liquid nitrogen cold trap, which consists of a 6-mm pyrex tube containing zinc shavings (Biogeochemical Laboratories, Indiana University). To minimize water adsorption to the glass, the glass transfer lines are wrapped in heating tape and heated up to 80°C. The cryogenically collected water is converted to hydrogen by reduction with Zn at 500°C for 30 min (Coleman et al., 1982) and the hydrogen gas is then measured on a VG PRISM II isotope ratio mass spectrometer.

Following Dennis et al. (1997, 2001), the efficiency and the precision of our electromagnetic crushing cell was tested with three types of samples: (1) laboratory standard water (LSTDW) (1 and 2 μl) sealed in glass capillaries, (2) LSTDW water crushed together with anhydrous calcite (Iceland Spar), and (3) the upper few millimeters of modern, actively growing stalagmites for which we also have measured the δD values of drip waters (Fleitmann et al., 1999). The results indicate that the total analytical precision is approximately ±3‰ and thus very similar to the precision given by Dennis et al. (1997, 2001) for the same method of extraction. Furthermore, duplicate measurements of speleothem fluid inclusions (Fig. 2) indicate a good reproducibility and underline the reliability of the vacuum-crushing method. The average standard deviation for 18 duplicate δD_{FI} samples also averages ±3‰ (Fig. 2).

Table 1
U and Th isotope concentrations with 2σ errors and calculated ages for Hoti Cave speleothems

Sample	Depth [cm]	Concentration ^{238}U		Concentration ^{232}Th		Concentration ^{230}Th		δ^{234}U		Age	
		μg/g	±	ng/g	±	pg/g	±	‰	±	yr	±yr
H1	Top	1.627	0.003	0.139	0.001	18.96	0.125	311.0	3.9	82,460	1215
H1	Bottom	1.344	0.004	0.380	0.007	14.95	0.284	305.4	4.8	77,620	2545
H4	1.0	1.148	0.005	5.080	0.022	14.91	0.097	202.0	6.6	112,900	2700
H4	4.3	1.646	0.014	4.832	0.047	22.52	0.293	212.5	9.3	121,600	5200
H4	35.0	0.713	0.001	0.807	0.004	9.037	0.080	157.1	3.8	116,900	2600
H4	57.0	0.594	0.001	3.563	0.009	7.612	0.062	162.4	4.3	117,600	2600
H4	84.0	0.593	0.001	0.276	0.003	7.844	0.110	191.3	5.7	119,000	4400
H5	0.5	3.429	0.009	200.340	2.200	5.530	0.150	498.2	6.3	6220	180
H5	2.5	9.204	0.052	56.350	0.680	13.44	0.260	517.6	5.9	6490	160
H5	6.5	5.080	0.007	8.097	0.020	8.740	0.038	617.8	3.6	7280	50
H5	9.8	4.031	0.010	10.397	0.076	7.611	0.077	617.5	6.8	8000	119
H5	13.5	4.510	0.014	7.093	0.035	8.461	0.070	605.2	6.1	8030	110
H5	16.0	4.313	0.011	10.924	0.083	7.982	0.087	592.8	6.5	7970	124
H5	17.6	4.157	0.020	21.934	0.323	8.369	0.223	590.1	13.2	8660	317
H5	20.5	4.002	0.006	22.210	0.040	7.610	0.040	599.5	8.0	8100	70
H5	23.5	4.371	0.014	15.190	0.180	8.390	0.300	593.9	9.5	8260	360
H5	25.5	3.904	0.032	14.650	0.250	8.110	0.160	582.6	9.8	9020	260
H5	29.5	4.566	0.016	91.640	0.810	10.32	0.170	634.2	8.8	9270	210
H5	32.5	5.057	0.010	63.406	0.451	10.92	0.091	546.5	4.8	9460	112
H5	35.0	4.201	0.006	40.810	0.100	9.813	0.036	642.0	2.3	9710	50
H5	40.0	4.091	0.006	10.261	0.037	8.945	0.045	547.5	3.9	9770	80
H5	43.5	3.097	0.007	22.709	0.166	7.147	0.084	584.2	7.3	10,000	173
H5	45.7	3.448	0.007	0.472	0.003	7.786	0.104	577.5	4.9	9940	175
H5	48.0	3.537	0.011	24.800	0.250	8.020	0.220	578.8	8.5	9860	350
H5	49.8	4.244	0.010	5.891	0.044	9.670	0.096	564.8	5.2	10,100	145
H5	53.5	4.256	0.012	0.591	0.006	10.60	0.147	613.6	8.4	10,760	220
Flowstone	6.0	0.253	0.001	4.757	0.031	3.334	0.043	164.7	11.4	122,200	5400
Flowstone	8.0	0.272	0.002	13.751	0.179	3.923	0.098	234.6	9.6	125,260	7760
Flowstone	72.5	0.318	0.001	19.780	0.130	3.595	0.043	252.6	5.6	82,000	2000
Flowstone	128.5	0.282	0.001	14.106	0.078	3.927	0.034	194.5	5.5	125,700	3170
Flowstone	178.5	0.299	0.001	5.665	0.052	3.890	0.066	215.4	6.9	110,200	4400
H10	Top	2.262	0.004	0.888	0.006	3.559	0.041	317.4	3.9	8250	125
H10	Bottom	4.844	0.012	1.735	0.014	9.716	0.653	375.6	5.5	10,150	760
H11	Top	8.339	0.020	0.721	0.005	12.84	0.108	308.3	4.4	8130	105
H11	Bottom	6.007	0.034	0.357	0.003	10.27	0.132	308.6	20.9	9060	285
H12	8.5	1.465	0.004	6.939	0.054	0.099	0.002	386.7	5.4	230	7
H12	15.1	1.673	0.003	14.036	0.190	0.214	0.009	390.8	5.1	450	22
H12	22.1	1.453	0.003	4.240	0.032	0.206	0.004	389.4	5.4	630	18
H12	33.8	1.053	0.002	1.254	0.010	0.280	0.005	369.3	5.7	1280	29
H12	37.2	1.344	0.002	7.624	0.057	0.441	0.007	375.1	4.9	1490	32
H12	39.1	1.580	0.003	17.889	0.148	0.607	0.008	392.2	5.7	1630	26
H12	40.0	2.739	0.007	19.015	0.155	0.984	0.016	376.7	5.9	1610	37
H12	57.1	1.805	0.005	21.046	0.166	1.034	0.015	380.7	6.4	2560	50
H12	59.5	1.956	0.005	24.174	3.193	2.156	0.026	364.7	5.4	5260	86
H12	63.8	2.145	0.006	28.325	0.376	2.562	0.044	344.5	8.0	5800	138
H12	66.0	1.786	0.004	4.180	0.060	2.043	0.025	342.3	5.2	5780	99
H12	74.4	1.885	0.005	18.746	0.144	2.204	0.034	330.5	6.1	5800	120
H12	76.0	1.763	0.004	9.509	0.087	2.118	0.022	330.9	5.1	6070	93
H13	1	0.26	0.000	0.52	0.004	4.136	0.065	347.9	6.3	129,000	4900
H13	9.5	0.3202	0.0003	0.258	0	5.04	0.01	359.1	2.9	124,260	720
H13	20	0.318	0.0002	0.682	0.001	5.04	0.02	365.7	2.6	124,300	900
H13	30	0.2514	0.0003	0.755	0.002	4.07	0.02	382.1	3.1	126,200	1300
H13	50	0.2923	0.0003	0.209	0.001	4.68	0.03	361.8	5.1	127,200	1600
H13	58	0.277	0.001	0.386	0.003	4.553	0.047	364.8	7.5	134,000	4200
H13	70	0.2876	0.0003	0.468	0.001	4.56	0.02	358.3	3.0	125,800	1000
H13	76	0.271	0.0002	1.097	0.004	4.32	0.03	359.6	3.0	126,600	1700
H13	81.7	0.2707	0.0003	0.258	0.001	4.32	0.02	357.3	3.3	127,510	1300
H13	112	0.48	0.001	0.786	0.006	7.631	0.061	372.9	0.7	124,000	2700
H13	120	0.6616	0.0005	0.353	0.001	10.61	0.05	371.8	2.0	125,900	1100
H13	131.5	2.1399	0.0032	0.606	0.002	34.83	0.14	385.8	2.8	126,800	1100
H13	138	3.1676	0.0035	<0.1	×	52.96	0.27	418.7	2.8	126,900	1300

Table 1 (*continued*)

Sample	Depth [cm]	Concentration ^{238}U		Concentration ^{232}Th		Concentration ^{230}Th		δ^{234}U		Age	
		μg/g	±	ng/g	±	pg/g	±	‰	±	yr	±yr
H13	143.5	2.1862	0.0026	3.484	0.007	36.68	0.12	419.1	2.6	127,600	900
H13	150.2	0.2238	0.0002	3.339	0.012	4.14	0.04	315.0	5.4	184,600	4300
H13	155	0.12	0.000	1.174	0.011	2.181	0.046	312.1	10.2	180,000	12,800
H13	160	0.43	0.001	1.019	0.008	8.355	0.08	345.6	0.8	197,000	7400
H13	184	0.245	0.001	4.895	0.04	4.594	0.054	329.7	0.7	187,000	9000
H13	188	0.186	0.000	1.237	0.009	3.524	0.029	323.7	0.6	194,000	6800
H13*	225	0.591	0.001	0.398	0.004	12.33	0.181	232.7	4.3	387,000	59,600
H13	238	0.537	0.001	0.303	0.002	10.71	0.091	227.6	0.4	308,000	20,600
H13	249	0.428	0.001	1.292	0.01	8.669	0.088	232.1	0.4	325,000	27,200
H13	262	0.369	0.001	0.531	0.004	7.424	0.056	242.8	0.7	299,000	18,600
H13*	270	0.425	0.001	3.114	0.024	8.895	0.088	244.2	7.1	366,000	34,600
H13	290	1.351	0.003	2.204	0.016	27.33	0.208	237.5	0.6	315,000	20,900
H14	1	1.6	0.003	2.541	0.018	2.415	0.025	605.9	1.1	6410	90
H14	5.2	1.978	0.008	1.051	0.008	3.206	0.046	627.6	2.5	6820	140
H14	5.9	2.305	0.005	0.727	0.005	3.798	0.035	621.9	1.4	6970	90
H14	15.3	3.111	0.012	0.66	0.009	5.226	0.12	614.3	2.4	7150	230
H14	16	2.642	0.006	0.459	0.004	4.492	0.043	615.8	1.4	7230	100
H14	20.2	1.637	0.004	0.382	0.003	2.979	0.036	613.2	1.4	7760	130
H14	21.2	1.98	0.004	1.292	0.011	3.578	0.052	609.3	1.4	7720	140
H14	28.4	2.035	0.005	0.737	0.01	3.726	0.048	609.2	1.4	7830	130
H14	30.1	1.247	0.002	0.197	0.001	2.314	0.025	591.8	1.2	8040	120
H14	30.5	1.733	0.003	0.189	0.002	3.175	0.043	579.4	1.1	7990	140
H14	32.8	2.108	0.004	1.481	0.01	4.041	0.035	588.0	1.1	8320	100
H14	40.5	2.208	0.007	2.058	0.017	4.269	0.041	575.0	1.8	8470	130

* Not shown in Figure 3.

Results

Age data

Uranium series ages of almost all stalagmites are with one exception (flowstone) in stratigraphic order. The flowstone shows a wide spread in ages ranging from 82,000 to 126,000 yr. (Fig. 3), but was very likely deposited during marine oxygen isotopic stage (MIS) 5e (~125,000 yr ago) because it underlies the precisely
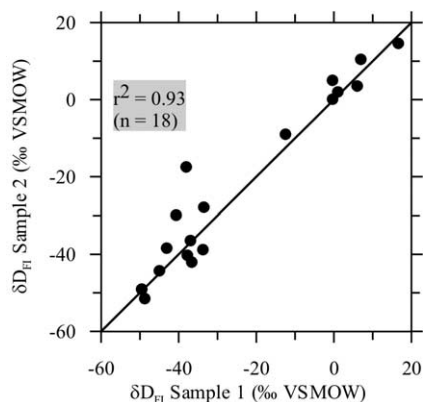

Fig. 2. Comparison of duplicate fluid inclusion analysis of stalagmites from Northern (*n* = 14) and Southern Oman (*n* = 4). Results of fluid inclusions analyses performed on stalagmites from Southern Oman are not included in this study.

dated stalagmite H4 and because three U/Th samples at 60–80 and 1270–1300 mm were dated at 122,000 ± 5400, 125,260 ± 7700 and 126,000 ± 3200 yr (see discussion in Burns et al., 1998). Age data of all stalagmites are shown in Figure 3 (see also Table 1) and indicate five distinct periods of speleothem deposition (Burns et al., 1998, 2001), occurring from 6000 to 10,500, 78,000 to 82,000, 117,000 to 130,000, 180,000 to 210,000, and 300,000 to 330,000 yr ago. Periods of speleothem deposition in Hoti Cave coincide with peak interglacial intervals equivalent to the early to middle Holocene as well as MIS 5a, 5e, 7a, and 9. The longest record from a single speleothem, stalagmite H13, comprises three periods of growth, corresponding to MIS 5e, 7a, and 9. A precise estimation of the duration of the MIS 7a and 9 growth intervals is difficult due to large U/Th age uncertainties, but we suggest that these periods last not longer than 5000 to 10,000 yr. The early to middle Holocene pluvial period and MIS 5e can serve as an analogue example for the two older intervals MIS 7a and 9, where age uncertainties vary between 7000 and 30,000 yr (Fig. 3).

Oxygen isotope composition of speleothem calcite

The composite oxygen isotope record of all Hoti Cave speleothems is shown in Figure 4a. $\delta^{18}O_C$ values of present-day stalagmites (H2, H3, and H12) range from −2.6 to
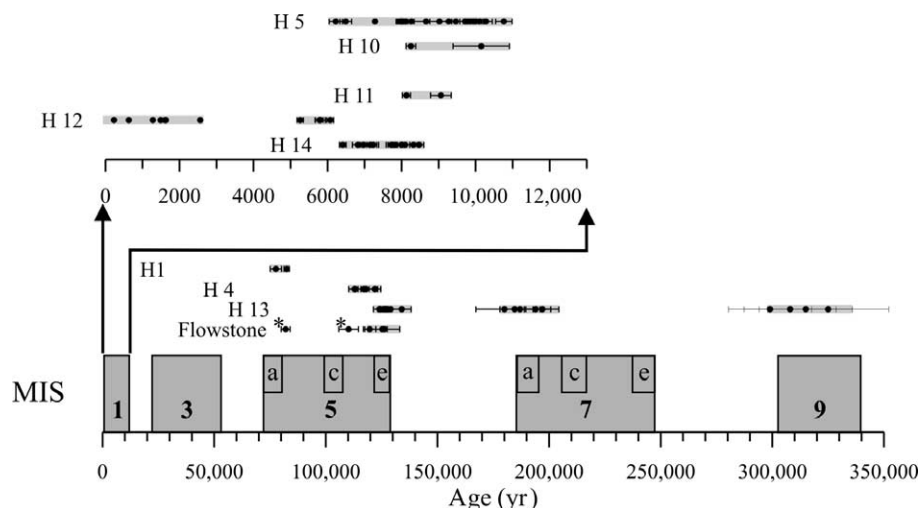
Fig. 3. Range of uranium-series dated stalagmites with associated age uncertainties (error bars) in Hoti Cave (see Table 1 for details). Gray-shaded areas mark the duration of growth. Speleothem growth in Hoti Cave occurred mainly during peak interglacial periods equivalent to the early to middle Holocene and marine oxygen isotope stages (MIS) 5a, 5e, 7a, and 9. No speleothem growth occurred during the intervening periods. Flowstone age data marked with a star symbol are unreliable (see text for further details).

−1.1‰. In contrast, stalagmites deposited during interglacial pluvial periods exhibit $\delta^{18}O_C$ values from −8 to −4‰. The composite oxygen isotope record reveals differences in $\delta^{18}O_C$ between individual interglacial periods. $\delta^{18}O_C$ values of stalagmites deposited during the early to middle Holocene and MIS 5a generally vary between −6.5 and −4.0‰, whereas MIS 5e, 7a, and 9 speleothems show lower $\delta^{18}O_C$ values, mostly ranging between −8 and −5‰, with some values as low as −12‰. The lowest $\delta^{18}O_C$ values, from −12 to −9‰, were measured in samples from the flowstone, which was deposited during MIS 5e. Four stalagmites (H4, H5, H13, and H14) show a large positive shift of 3 to 4‰ in $\delta^{18}O_C$ within their uppermost 1 to 4 cm (Fig. 4a), marking rapid transitions from wet to dry periods.

Hydrogen isotope composition of speleothem fluid inclusions

Overall, δD_{FI} values vary between −53 and +19‰ (VSMOW) (Fig. 4b). δD_{FI} values from present-day stalagmites (H2 and H12) fall to the more positive end of this range, varying between −14 and 19‰ (VSMOW), whereas δD_{FI} values from peak interglacial samples (H4, H5, H13, H14, and flowstone) are generally isotopically lighter, with values varying from −60 to −20‰ (VSMOW). The exception is one sample from the upper part of stalagmite H4 at the termination of MIS 5e that has a δD_{FI} value of +2‰ (VSMOW). A sharp shift to more positive isotopic values also occurs in the oxygen isotope record, where $\delta^{18}O_C$ shifts from approximately −5 to −0.5‰ within a few millimeters. Stalagmite H1 (MIS 5a) is not suitable for fluid-inclusion analyses due to its porous carbonate textures.

Discussion

Isotopic composition of rainfall and local groundwater

The present-day isotopic composition of precipitation and local groundwater as well as cave drip waters in Northern Oman must be known before δD_{FI} and $\delta^{18}O_C$ values of fossil speleothems can be interpreted. Although no long-term precipitation or cave drip-water isotope records exist in Northern Oman, a relatively large number of isotope analyses of rainfall samples were carried out in a number of previous studies (e.g., Gibb, 1976; Stanger, 1986; Clark, 1987; Macumber et al., 1995; Weyhenmeyer et al., 2000, 2002; Matter, 2001). Weyhenmeyer et al. (2000, 2002) showed that modern precipitation from northern moisture sources (Mediterranean frontal systems) and from southern moisture sources (Arabian Sea and Bay of Bengal) differ greatly in their isotopic composition. As shown in Figure 5, precipitation from a northern moisture source ranges from −4.5 to +1.0‰ in $\delta^{18}O$ and from −25 to +5‰ in δD (Weyhenmeyer et al., 2000, 2002), whereas precipitation from a southern source is much more depleted, with $\delta^{18}O$ values varying from −10 to −2‰ and δD values from −75 to −15‰. Furthermore, the two sources of moisture define separate Local Meteoric Water Lines, a Northern Local Meteoric Water Line (N-LMWL; $\delta D = 5.0\ \delta^{18}O + 10.7$) and a Southern Local Meteoric Water Line (S-LMWL; $\delta D = 7.1\ \delta^{18}O − 1.1$) (Weyhenmeyer et al., 2000, 2002). The isotopic compositions of young, tritium-containing groundwater samples ($n = 11$) in the vicinity of Hoti Cave and cave drip water samples ($n = 3$) plot between both local meteoric water lines, indicating that precipitation from both moisture sources recharges local
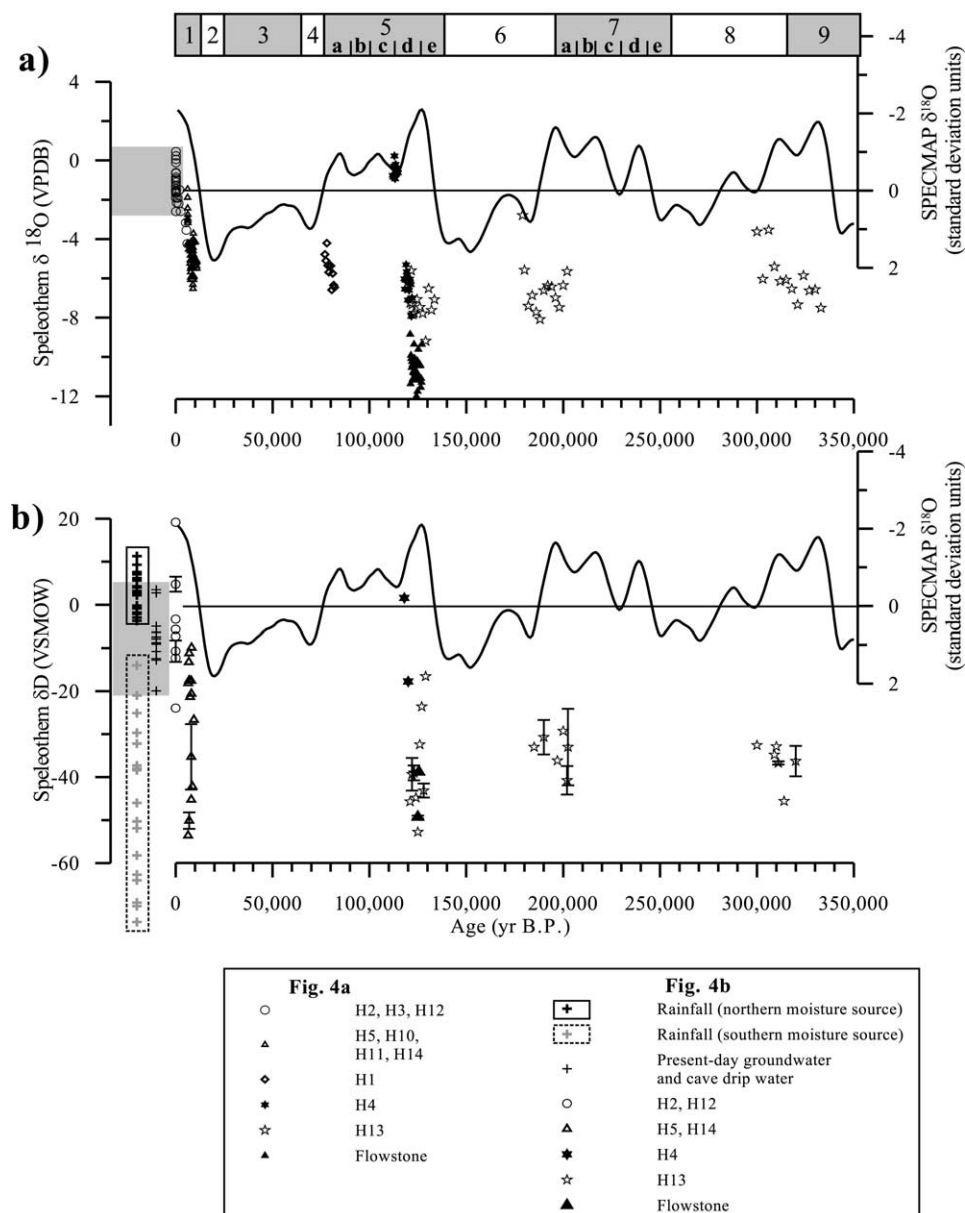
Fig. 4. (a) Composite oxygen isotope record for Hoti Cave. Gray-shaded area marks the range of $\delta^{18}O$ values of present-day stalagmites. Samples H2 and H3 as well as the top of H12 are modern; all other ages are based on U/Th data (modified from Burns et al., 2000). Also shown is the SPECMAP (Imbrie et al., 1990) marine oxygen isotope curve and MIS numbers. Note that two U/Th ages (387,000 ± 59,600 and 366,000 ± 34,600 yr) with large age uncertainties of stalagmite H13 are not displayed. (b) Composite hydrogen isotope record for Hoti Cave (including the results of duplicate samples, black dots with error bars). The gray-shaded area marks the isotopic range of present-day groundwater and cave drip waters. Additionally shown is the hydrogen isotope composition of rainfall originating from a northern moisture source (black line rounded rectangle) and precipitation originating from a southern moisture source (dashed rounded rectangle). Also shown is the SPECMAP marine oxygen isotope curve and marine oxygen isotope stage numbers (Imbrie et al., 1990).

groundwater (Weyhenmeyer, 2000, 2002; Matter, 2001; Fleitmann, 2001) (Fig. 5). Based on the stable isotope analysis of 191 groundwater samples, Weyhenmeyer et al. (2000) developed a Northern Oman Groundwater Line (N-OGL; $\delta D = 5.3\ \delta^{18}O + 2.7$) that plots between both Local Meteoric Water Lines. Finally, isotopic as well as geochemical data reveal that local groundwater shows no, or only minor, signs of evaporation (Weyhenmeyer et al., 2002; Matter, 2001).

Isotopic composition of speleothems

$\delta^{18}O_C$ values of actively growing stalagmites in Hoti cave range from −2.6 to −1.1‰ (Fig. 4a) and, thus, are very close to values expected for isotopic equilibrium deposition of speleothem calcite with its parent drip water ranging from −1.4 to −0.2‰ at measured cave air temperatures of 25°–27°C. Also δD_{FI} values of modern stalagmites are within the measurement error of δD values of present-
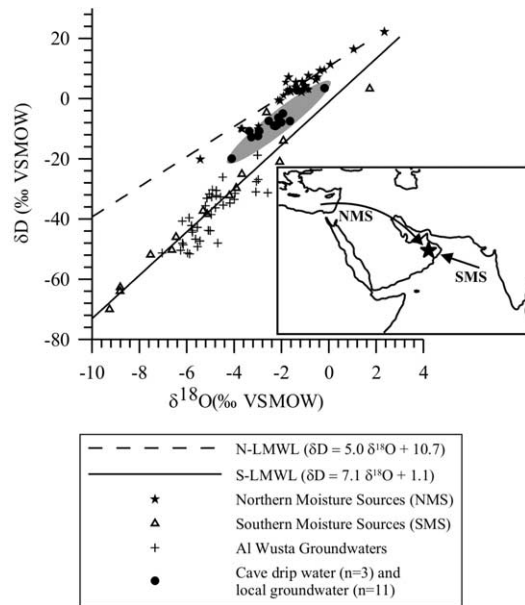
Fig. 5. Hydrogen and oxygen isotope composition of Rainfall (Weyhenmeyer et al., 2000, 2002; Matter, 2001) from various rainfall events occurring between 1995 and 1999 in Northern Oman. Two Local Meteoric Water Lines (LMWL) exist, the Northern-LMWL characterizing precipitation originating from a northern moisture source (Mediterranean frontal systems, NMS) and the Southern-LMWL for precipitation (tropical Indian Ocean cyclones, SMS) from a southern moisture source. Cave drip waters ($n = 3$) as well as groundwater from springs and wells in the vicinity of Hoti Cave are also plotted (Matter, 2001; Fleitmann, 2001). The gray-shaded area marks the isotopic range of ground- and drip water samples. Groundwater samples from the Al Wusta region, where rainfall solely originates from a southern moisture source, are also shown (Macumber et al., 1995).

day groundwater and cave drip waters (Fig. 4b). Therefore, active stalagmites in Hoti Cave closely reflect, even under present-day arid climate conditions, the isotope composition of cave seepage water and local groundwater, respectively, which is recharged by precipitation originating from a mixture of northern (Mediterranean) and southern moisture (Indian Ocean) sources (Fig. 5). Speleothems deposited during peak interglacial periods have isotopically much lower δD_{FI} and $\delta^{18}O_C$ values (Figs. 4a and b). The observed difference between active and fossil stalagmites is too large to be explained by changes in air temperature and/or cave air temperature for two reasons:

(1) Higher cave air temperature influences solely the temperature-dependent fractionation of ^{18}O during calcite precipitation ("*cave temperature effect*" approximately $-0.25‰$ per $1°C$ increase; O'Neil et al., 1969), but not δD_{FI} values. Furthermore, a depletion of $1‰$ in $\delta^{18}O_C$ would require a temperature increase of $4.5°C$, but marine oxygen isotope records from the Arabian Sea (e.g., Murray et al., 1992) and climate models (COHMAP, 1988) as well as groundwater data (Weyhenmeyer et al., 2000) demonstrate that temperatures during the early and middle Holocene were within $1°–2°C$ of present-day temperatures.

(2) The so-called "*temperature effect*" of $\delta^{18}O$ and δD in

precipitation is attenuated in tropical areas and overprinted by the so called "*amount effect*" (Daansgard, 1964) that describes the negative correlation of $\delta^{18}O$ and δD with the amount precipitation.

After temperature-related effects are ruled out, the most plausible explanation for very low $\delta^{18}O_C$ and δD_{FI} values of fossil speleothems is a change in the source of moisture at peak interglacial periods. To test this hypothesis, the average isotopic composition of paleogroundwater was calculated for the individual periods of speleothem deposition. Whereas δD_{FI} values directly reflect the isotopic composition of paleogroundwater, $\delta^{18}O$ values must be calculated from measured $\delta^{18}O_C$ values using the calcite-water fractionation equation ($10^3\ln \alpha = 2.78(10^6T^{-2}) -2.89$; Friedman and O'Neil, 1977), assuming a cave air temperature between $25°$ and $27°C$. On a $\delta^{18}O$ versus δD plot reconstructed peak interglacial groundwater values plot very close to the S-LMWL, whereas recent to subrecent and MIS 5e/5c (stalagmite H4) values plot closer to the N-OGL (Fig. 6). We conclude that during each pluvial period, a much greater percentage of the total moisture brought to the region originated in the Indian Ocean.

Additional evidence for the hypothesis that precipitation from a tropical southern moisture source recharged groundwater during peak interglacial periods comes from the comparison with groundwater in the Al Wusta area (Macumber, 1995), which is exclusively recharged by precipitation originating from a southern moisture source. The isotope composition of Al Wusta groundwater overlaps reconstructed peak interglacial isotope values of paleogroundwater (Fig.
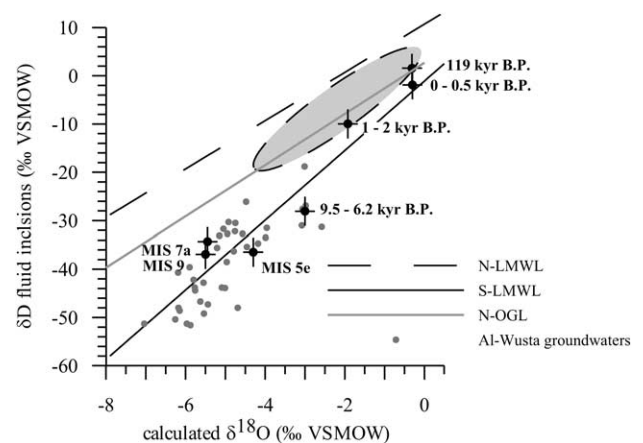

Fig. 6. δD versus $\delta^{18}O$ plot of the reconstructed isotopic composition of cave drip waters and meteoric precipitation respectively for intervals of speleothem deposition in Northern Oman (black dots with error bars). The reconstruction is based on δD_{FI} values of speleothem fluid inclusions and calculated $\delta^{18}O$ values of cave drip water (see text for details). Horizontal error bars show the possible range in $\delta^{18}O$ assuming a cave air temperature of $26 \pm 1°C$. Vertical error bars show the 2σ error ($\pm 3‰$) for δD measurements of speleothem fluid inclusions (see text for details). Gray-colored circles show the isotopic composition of Al Wusta groundwater (Macumber et al., 1995). Gray-shaded area shows the isotopic range of local young, tritium-containing groundwater and cave drip water (Matter, 2001).

6). Thus, highly depleted isotope values of peak interglacial stalagmites clearly document that precipitation from a southern moisture source predominantly recharged groundwater during the early to middle Holocene, MIS 5a, 5e, 7a, and 9.

Finally, the question arises what type of precipitation recharged groundwater during peak interglacial periods in Northern Oman? Two types of precipitation originate from a southern moisture source; these are tropical cyclones and monsoon precipitation, both of which are highly depleted in δD and $\delta^{18}O$. For instance, groundwater in the Al Wusta region where precipitation originates exclusively from tropical cyclones have average values of $-38.5‰$ for δD and $-4.9‰$ for $\delta^{18}O$, almost identical to those of monsoon precipitation in New Delhi (28.5 °N; 77.2 °E; 212 m above sea level; 1960–1995). Stable isotope composition of summer monsoon precipitation averages $-45.6‰$ for δD and $-6.9‰$ for $\delta^{18}O$ (IAEA/WMO, 1998). From there, depleted peak interglacial $\delta^{18}O_C$ and δD_{FI} values may indicate that either the Indian Ocean monsoon and/or more frequent tropical cyclones could have recharged groundwater during the Holocene, MIS 5a, 5e, 7a, and 9. However, it is more likely that monsoon precipitation recharged groundwater during peak interglacial periods, because early to middle Holocene paleolake records from throughout northern Africa and India (e.g., McClure, 1976; Street-Perrott and Perrott, 1990; Gasse, 2000, 2002) indicate that the intertropical convergence zone and the associated monsoon rainfall belt were located much further north of its present-day position. Further evidence for this assumption comes, for instance, from fossil groundwaters (12,800–3600 ^{14}C yr B.P.) from northern Mali (West Africa), which have much lower δD, and $\delta^{18}O$ values compared to modern precipitation (Fontes et al., 1993). Fontes et al. (1993) concluded a northward movement of the ITCZ by approximately 500 km during the early to middle Holocene. Again, such isotopically depleted isotope composition is characteristic for strong convective rainfall often developing along the ITCZ. Thus, during the early to middle Holocene and during MIS 5a, 5e, 7a, and 9, when the ITCZ was located further north of its present position, monsoon rainfall was the primary source of groundwater recharge, whereas precipitation from a northern, Mediterranean moisture source likely decreased or ceased in Northern Oman.

Conclusions

Stable isotope compositions (δD_{FI} and $\delta^{18}O_C$) of modern stalagmites accurately record, even under arid climate conditions, the stable isotope composition of local groundwater and precipitation, respectively. Today, precipitation in Northern Oman originates from both a northern (Mediterranean) and southern (Indian Ocean) moisture source. δD_{FI} and $\delta^{18}O_C$ values of fossil stalagmites, deposited during the early to middle Holocene, MIS 5a, 5e, 7a, and 9, are much more negative than values of modern stalagmites. Reconstructed groundwater values for these intervals, based on δD_{FI} and $\delta^{18}O_C$ values, indicate that groundwater was predominately recharged by monsoon precipitation from a southern (Indian Ocean) moisture source, when the ITCZ and associated the monsoon rainfall belt reached Hoti Cave in Northern Oman. This study shows that hydrogen isotope analyses of speleothem fluid inclusions in combination with oxygen isotope analyses of speleothem calcite enable the reconstruction of the isotopic composition of paleogroundwater and paleoprecipitation for the last 330,000 yr.

References

Anderson, D.M., Prell, W.L., 1993. A 300 kyr record of the upwelling off Oman during the Late Quaternary: evidence of the Asian southwest monsoon. Paleoceanography 8, 193–208.

Burns, S.J., Fleitmann, D., Matter, A., Neff, U., Mangini, A., 2001. Speleothem evidence from Oman for continental pluvial events during interglacial periods. Geology 29, 623–626.

Burns, S.J., Matter, A., Norbert, F., Mangini, A., 1998. Speleothem-based paleoclimate record from northern Oman. Geology 26, 499–502.

Clark, I.D., Fritz, P.E., Quinn, O.P., Rippon, P.W., Nash, H., bin Ghalib al Said, B., 1987. Modern and fossil groundwater in an arid environment: a look at the hydrogeology of southern Oman. In: Use of Stable Isotopes in Water Resources Development. International Atomic Energy Agency Symposium, 299, March 1987, Vienna. pp. 167–187.

Clemens, S.C., Prell, W.L., 1990. Late Pleistocene variability of Arabian Sea summer monsoon winds and continental aridity: eolian records from the lithogenic component of deep-sea sediments. Paleoceanography 5, 109–145.

Clemens, S.C., Prell, W.L., Murray, D., Shimmield, G., Weedon, G., 1991. Forcing mechanisms of the Indian Ocean monsoon. Nature 353, 720–725.

COHMAP Members, 1988. Climatic changes of the last 18,000 years: observation and model simulations. Science 241, 1043–1052.

Coleman, M.L., Shepard, T.J., Rouse, J.E., Moore, G.R., 1982. Reduction of water with zinc for hydrogen isotope analysis. Analytical Chemistry 54, 993–995.

Dansgaard, W., 1964. Stable isotopes in precipitation. Tellus 16, 436–468.

Dennis, P.F., Rowe, P.J., Atkinson, T.C., 1997. The stable isotope composition of palaeoprecipitation and palaeogroundwaters from speleothem fluid inclusions. International Symposium on Isotope Techniques in the Study of Past and Current Environmental Changes in the Hydrosphere and the Atmosphere. International Atomic Energy Agency Report IAEA-SM-349/44.

Dennis, P.F., Rowe, P.J., Atkinson, T.C., 2001. The recovery and isotopic measurement of water from fluid inclusions in speleothems. Geochimica et Cosmochimica Acta 65, 871–884.

Fleitmann, D., 2001. Annual to millennial Indian Ocean monsoon variability recorded in Holocene and Pleistocene stalagmites from Oman. Ph.D. thesis, University of Bern, Switzerland.

Fleitmann, D., Burns, S.J., Matter, A., 1999. Stable isotope study of the active water-carbonate system in caves in Oman: a test of applicability to paleoclimate studies. Eos Trans. AGU, 80, Fall Meet. Suppl., Abstract OS22B-12.

Fontes, J.-C., Gasse, F., Andrews, J.N., 1993. Climatic conditions of Holocene groundwater recharge in the Sahel zone of Africa in: Isotope Techniques in the Study of Past and Current Environmental Changes in the Hydrosphere and the Atmosphere, IAEA-SM-329/59, pp. 231–248.

Frank, N., Braun, M., Hambach, U., Mangini, A., Wagner, G., 2000. Warm period growth of travertine during the last interglaciation in southern Germany. Quaternary Research 54, 38–48.

Friedman, I., O'Neil, J.R., 1977. Compilation of stable isotope fractionation factors of geochemical interest. In Data of Geochemistry, sixth edition, United States Geological Survey, Washington DC, Chapter KK, Professional Paper 440-KK.

Gasse, F., 2000. Hydrological changes in the African tropics since the Last Glacial Maximum. Quaternary Science Reviews 19, 189–213.

Gasse, F., 2002. Diatom-inferred salinity and carbonate oxygen isotopes in Holocene waterbodies of the western Sahara and Sahel (Africa). Quaternary Science Reviews 21, 737–767.

Gibb, Sir A., Partners 1976. Water resources survey of northern Oman. Internal Report, Ministry of Water Resources, Sultanate of Oman.

Harmon, R.S., Schwarcz, H.P., O'Neil, J.R., 1979. D/H ratios in speleothem fluid inclusions: a guide to variations in the isotopic composition of meteoric precipitation. Earth and Planetary Science Letters 42, 254–266.

Hastenrath, S., 1985. Climate and Circulation of the Tropics. Reidel, Boston.

IAEA/WMO 1998. Global Network for Isotopes in Precipitation. The GNIP Database. Release 3, October 1999. URL: http://www.iaea.org/programs/ri/gnip/gnipmain.htm.

Imbrie, J., et al. 1990. SPECMAP Archive 1. IGB.P. PAGES/World Data Center-A for Paleoclimatology Data Contribution Series 90–001. NOAA/NGDC Paleoclimatology Program, Boulder, CO.

Ivanovich, M., Harmon, R.S., 1993. Uranium Series Disequilibrium: Applications to Environmental Problems. Clarendon, Oxford.

Kendall, A.C., Broughton, P.L., 1978. Origin of Fabrics in Speleothems composed of columnar calcite crystals. Journal of Sedimentary Petrology 48, 519–538.

Macumber, P.G., Barghash bin Ghalib Al-Said, Kew, G.A., and Tennakonn, T.B. 1995. Hydrogeologic implications of a cyclonic rainfall event in central Oman. In: Groundwater Quality, Nash, H., McCall, G.J.H., (Eds.). Chapman & Hall, London, pp. 87–97.

Matter, J.M., 2001. Geochemical evolution and hydrodynamics of groundwater in the Alluvial aquifer of the Dakhiliya area, Sultanate of Oman. Ph.D. thesis, ETH-Zürich, Switzerland.

Matthews, A., Ayalon, A., Bar-Matthews, M., 2000. D/H ratios of fluid inclusions of Soreq cave (Israel) speleothems as a guide to the Eastern Mediterranean Meteoric Line relationships in the last 120 ky. Chemical Geology 166, 183–191.

McClure, H.A., 1976. Radiocarbon chronology of late Quaternary lakes in the Arabian Desert. Nature 263, 755–756.

Murray, D.W., Prell, W.L., 1992. Late Pliocene and Pleistocene climatic oscillations and monsoon upwelling recorded in sediments from the Owen Ridge, northwestern Arabia Sea.. In Summerhayes, C.P., et al. (Eds.), "Upwelling Systems: Evolution since the Early Miocene." Geological Society, [London], pp. 301–321 Special Publication 64.

Neff, U., Burns, S.J., Mangini, A., Mudelsee, M., Fleitmann, D., Matter, A., 2001. Evidence for solar forcing of the Indian Monsoon in a high-resolution speleothem record from Oman. Nature 411, 290–293.

O'Neil, J.R., Clayton, R.N., Mayeda, T.K., 1969. Oxygen isotope fractionation in divalent metal carbonates. Journal Chemical Physics 51, 5547–5558.

Pedgely, D.E., 1989. Cyclones along the Arabian coast. Weather 24, 456–486.

Preusser, F., Radies, D., Matter, A., 2002. A 160 ka record of dune development and atmospheric circulation in Southern Arabia. Science 296, 2018–2020.

Schwarcz, H.P., Harmon, R.S., Thompson, P., Ford, D.C., 1976. Stable isotope studies of fluid inclusions in speleothems and their paleoclimatic significance. Geochimica et Cosmochimica Acta 40, 657–665.

Stanger, G., 1986. The hydrogeology of the Oman Mountains. Ph.D. thesis, Open University, UK.

Street-Perrott, F.A., Perrott, R.A., 1990. Abrupt climate fluctuations in the tropics: the influence of Atlantic circulation. Nature 343, 607–612.

Szabo, B.J., Haynes Jr., C.V., Maxwell, T.A., 1995. Ages of Quaternary pluvial episodes determined by uranium-series and radiocarbon dating of lacustrine deposits of Eastern Sahara. Palaeogeography, Paleoclimatology, Palaeoecology 113, 227–242.

Van Campo, E., Duplessy, J.C., Rossignol-Strick, M., 1982. Climatic conditions deduced from a 150-kyr oxygen isotope-pollen record from the Arabian Sea. Nature 296, 56–59.

Weyhenmeyer, C.E., Burns, S.J., Waber, H.N., Aeschbach-Hertig, W., Kipfer, R., Beyerle, R., Loosli, H., Matter, A., 2000. Cool glacial temperatures recorded by noble gases in a groundwater study from Northern Oman. Science 287, 842–845.

Weyhenmeyer, C.E., Burns, S.J., Waber, H.N., Macumber, P.G., Matter, A., 2002. Isotope study of moisture sources, recharge areas and groundwater flowpaths within the Eastern Batinah coastal plain, Sultanate of Oman. Water Resources Research 38, 1184 doi: 10.1029/2000WR000149,2002.

Yonge, C.J., 1982. Stable isotope studies of water extracted from speleothems. Ph.D. thesis, McMaster University, Canada.

Yonge, C.J., Ford, D.C., Gray, J., Schwarcz, H.P., 1985. Stable isotope studies of seepage water. Chemical Geology 58, 97–105.